First experiments probing the collision of parallel magnetic fields using laser-produced plasmas

M. J. Rosenberg, C. K. Li, W. Fox, I. Igumenshchev, F. H. Séguin, R. P. J. Town, J. A. Frenje, C. Stoeckl, V. Glebov, and R. D. Petrasso

Citation: Physics of Plasmas (1994-present) **22**, 042703 (2015); doi: 10.1063/1.4917248
View online: http://dx.doi.org/10.1063/1.4917248
View Table of Contents: http://scitation.aip.org/content/aip/journal/pop/22/4?ver=pdfcov
Published by the AIP Publishing

First experiments probing the collision of parallel magnetic fields using laser-produced plasmas

M. J. Rosenberg,[1,a)] C. K. Li,[1] W. Fox,[2] I. Igumenshchev,[3] F. H. Séguin,[1] R. P. J. Town,[4] J. A. Frenje,[1] C. Stoeckl,[3] V. Glebov,[3] and R. D. Petrasso[1]
[1]*Plasma Science and Fusion Center, Massachusetts Institute of Technology, Cambridge, Massachusetts 02139, USA*
[2]*Princeton Plasma Physics Laboratory, Princeton, New Jersey 08543, USA*
[3]*Laboratory for Laser Energetics, University of Rochester, Rochester, New York 14623, USA*
[4]*Lawrence Livermore National Laboratory, Livermore, California 94550, USA*

(Received 8 January 2015; accepted 30 March 2015; published online 8 April 2015)

Novel experiments to study the strongly-driven collision of parallel magnetic fields in $\beta \sim 10$, laser-produced plasmas have been conducted using monoenergetic proton radiography. These experiments were designed to probe the process of magnetic flux pileup, which has been identified in prior laser-plasma experiments as a key physical mechanism in the reconnection of anti-parallel magnetic fields when the reconnection inflow is dominated by strong plasma flows. In the present experiments using colliding plasmas carrying parallel magnetic fields, the magnetic flux is found to be conserved and slightly compressed in the collision region. Two-dimensional (2D) particle-in-cell simulations predict a stronger flux compression and amplification of the magnetic field strength, and this discrepancy is attributed to the three-dimensional (3D) collision geometry. Future experiments may drive a stronger collision and further explore flux pileup in the context of the strongly-driven interaction of magnetic fields. © *2015 AIP Publishing LLC*.
[http://dx.doi.org/10.1063/1.4917248]

I. INTRODUCTION

The dynamics of interacting and colliding plasmas carrying magnetic fields is a universal problem that appears at any boundary between magnetically separated regions. When magnetic fields are squeezed together in an anti-parallel configuration, field lines are prone to breaking and rearranging their topology in a manner that reduces the stored magnetic energy. This process of magnetic reconnection has been studied extensively in analytical theory,[1,2] computational studies,[3] spacecraft observations,[4] and laboratory experiments.[5,6] Recent experiments using laser-generated plasmas have explored magnetic reconnection in strongly-driven configurations,[7–11] where plasma inflows are a significant source of energy and the compression and amplification of magnetic fields are expected to play a significant role in the reconnection physics.[12] This strongly-driven reconnection occurs in some astrophysical environments, such as the dayside magnetopause[13] in the interaction between the solar wind and the Earth's magnetosphere. The compression of magnetic flux is also of astrophysical relevance, as magnetic fields tend to suppress hydrodynamic instabilities.[14]

Presented here are the first laboratory experiments designed to study magnetic field deformation and flux compression in the strongly-driven collision of *parallel* magnetic fields in a high-β plasma. Previous experiments driving the interaction of anti-parallel magnetic fields in high-β, laser-produced plasmas have demonstrated signatures of magnetic reconnection[7–10] and observed an extremely fast rate of magnetic flux annihilation.[8,11] The nominally super-Alfvénic reconnection has been attributed to the pileup of magnetic flux during the collision process, which amplifies the local magnetic field strength and Alfvén speed. In this strongly-driven system, where the bulk flow velocity is significantly larger than the Alfvén speed and, equivalently, ram pressure dominates magnetic pressure, the fields are forced together faster than they can naturally rearrange themselves. The present experiments provide a test bed for investigating the physics of flux pileup in a configuration where magnetic reconnection is prohibited by the parallel configuration of the colliding magnetic fields. These experiments are therefore critical in interpreting the related magnetic reconnection experiments, which in turn inform our understanding of magnetic reconnection dynamics in several astrophysical environments. In these experiments, it is observed that the magnetic flux is conserved and slightly compressed in the collision region. The observed flux compression and magnetic field amplification is not as great as is predicted by two-dimensional (2D) particle-in-cell (PIC) simulations. Thus, three-dimensional (3D) dynamics is proposed to be an important consideration.

This paper is organized as follows: Section II describes the experimental setup for studying the collision of parallel magnetic fields in laser-produced plasmas; Sec. III presents proton radiography images and measurements of the magnetic fields and magnetic flux; Sec. IV describes the comparison of experimental data to the predictions of 2D PIC simulations to deduce the key physics dictating the plasma dynamics and magnetic field evolution; and Sec. V presents concluding remarks.

[a)]Current address: Laboratory for Laser Energetics, University of Rochester, New York, USA. Electronic mail: mros@lle.rochester.edu

II. EXPERIMENTS

As is illustrated in Figure 1, self-generated magnetic fields are produced in the interaction of lasers with solid targets. A laser striking a foil perpendicularly gives rise to an expanding, hemispherical plasma bubble, with an electron density gradient directed towards the foil and an electron temperature gradient directed radially inward towards the center of the laser spot. The Biermann battery mechanism produces an azimuthal magnetic field, as $\frac{\partial B}{\partial t} \propto \nabla T_e \times \nabla n_e$. This field is advected radially outward along the perimeter of the plasma bubble during its expansion.

Laser-plasma experiments to study colliding parallel magnetic fields were conducted at the OMEGA laser facility.[15] In each experiment, depicted in Figure 2, two oppositely-directed 500-J, 1-ns laser pulses at a wavelength of 351 nm and with an 800-μm spot size were each incident on separate 5-μm-thick CH foils. Each laser-foil interaction generated an expanding, hemispherical plasma bubble, with ~0.5 MG toroidal magnetic fields advected with the expansion of the plasma bubble and concentrated at its perimeter.[16] Two parallel foils were separated by 1 mm in the direction normal to their surface and offset laterally. The laser spots were incident 0.7 mm from the edge of the foil such that symmetric plasma bubbles expanding from each surface would collide at a radius of 700 μm and an out-of-plane height of 500 μm. The expanding azimuthal magnetic field structures are parallel at the point where they interact. In some experiments, the relative timing (Δt) between the onset of the two interaction beams was non-zero in order to produce an asymmetric plasma bubble collision.

The interacting magnetic fields were imaged using monoenergetic proton radiography.[17,18] A spherical glass backlighter capsule with a 420-μm diameter and a 2 μm-thick wall, filled with 18 atm of D^3He gas, was imploded by 22 OMEGA lasers, delivering 11 kJ in a 1-ns pulse. This implosion generated an isotropic burst of monoenergetic 15-MeV protons from the D^3He fusion. The uniform fluence of protons was divided by a 150-μm-period Ni mesh into discrete

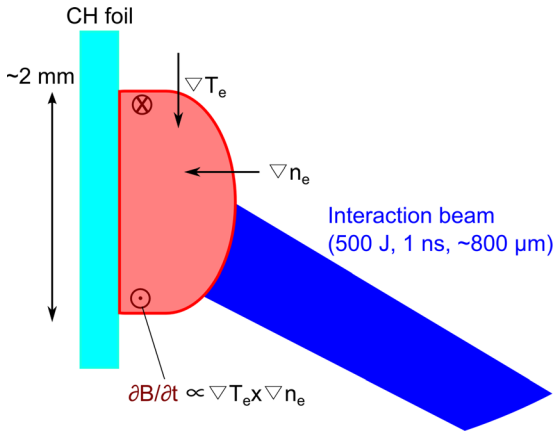

FIG. 1. Generation of magnetic fields in laser-foil interactions. The ablation of a CH foil produces an electron density gradient in the direction of the foil, while the laser profile generates an electron temperature gradient directed radially inward. Through the Biermann battery mechanism, an azimuthal magnetic field is generated, encircling the expanding, hemispherical plasma bubble.

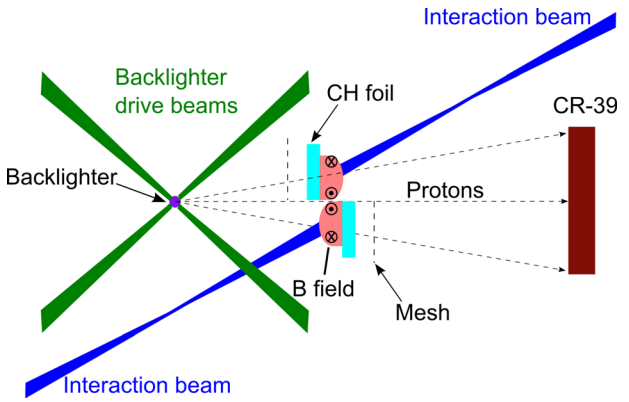

FIG. 2. Experimental setup for proton radiography of colliding plasmas carrying parallel magnetic fields. The distance between the backlighter capsule and the interaction point was 10 mm, while each foil was 0.5 mm from the center; the distance between the mesh and the foil was 2 mm for the backlighter-facing mesh and 2.5 mm for the detector-facing mesh. The distance between the backlighter and the detector was 270 mm, such that the magnification was M ~ 27. In some experiments, the relative timing (Δt) between the two interaction beams was non-zero in order to produce an asymmetric plasma bubble collision.

beamlets, which sampled the plasma. The proton beamlets were deflected by magnetic fields and their positions were recorded on the solid-state nuclear track detector CR-39. The measured deflection of each beamlet, as determined by the deviation in its position relative to an unperturbed grid, was used to infer the local path-integrated magnetic field strength ($|\int \mathbf{B} \times \mathbf{dl}|$). Two separate pieces of mesh, one for each target foil was used at different distances, one on the backlighter side of its foil, and one on the detector side, in order to avoid being struck by the incident laser. In separate experiments, the timing between the onset of the interaction beams and the onset of the backlighter drive beams was varied so that the backlighter protons sampled the plasma at different times in the collision process.

III. RESULTS

15-MeV-proton radiography images of colliding, laser-produced plasmas carrying parallel magnetic fields are shown in Figure 3. These images demonstrate the deflection of proton beamlets due to magnetic fields concentrated at the perimeter of the plasma bubbles and in their interaction. The plasma bubble at the top (bottom) half of each image has azimuthal magnetic fields that are oriented clockwise (counterclockwise) when looking toward the backlighter from the detector, and the proton beamlets are deflected radially outward (inward). This effect has been observed previously in laser-foil experiments with lasers incident on opposite sides of the same foil, but with no interaction between the plasma bubbles.[16] Where the plasma bubbles collide, the magnetic fields are parallel, both pointing to the left, deflecting protons downward in both cases.

The grid structure on each side of the image has a different apparent size due to the different magnifications of the two pieces of mesh. The mesh for the smaller-appearing bubble is 1.3 mm from the backlighter, while the mesh for the larger-appearing bubble is 0.75 mm from the backlighter. In some experiments, a light strip (deficit of protons) appears in

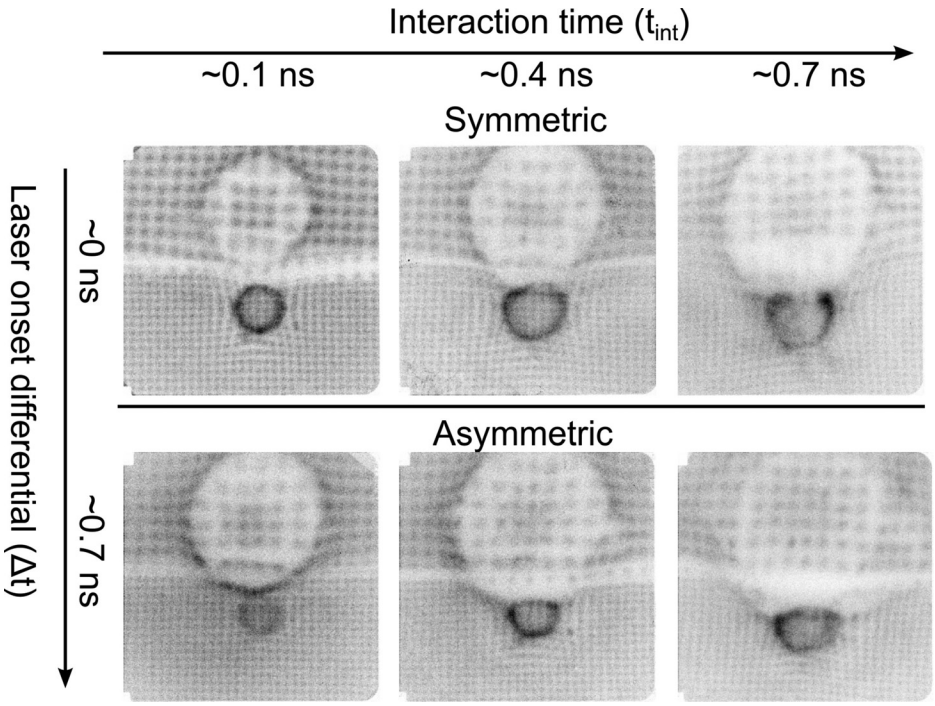

FIG. 3. 15-MeV-proton images at different times relative to the onset of the two interaction beams. The horizontal axis represents how long the two plasmas have been interacting (increasing t_{int}. to the right) for symmetric ($\Delta t = 0$) and asymmetric ($\Delta t = 0.7$ ns) experiments. Darker indicates more protons.

the center of the image, possibly due to the overlap of the two meshes, preventing proton transmission, or due to a slight charging of the mesh itself, which could create an electric field that deflects protons away from the edge of the mesh.

The time axes in Figure 3 are the duration of time since the plasmas began to interact (t_{int}.) and the difference in onset time between the two interaction beams (Δt). Experiments at $\Delta t = 0$ are symmetric, even though one bubble appears smaller and the other appears larger, due to the different magnetic deflections. Experiments at $\Delta t = 0.7$ ns are asymmetric, with the larger-appearing bubble actually larger, as it has had more time to expand. The timing was confirmed by the proton temporal diagnostic (PTD), which measures the absolute time of proton emission from the backlighter.[19]

The proton fluence structures evolve as a result of the generation, growth, and interaction of magnetic field structures. In the top half of the images, the apparent bubble size (the radius of high proton fluence) increases rapidly due to the radial expansion of the bubble and the strengthening of the path-integrated magnetic fields. In the bottom half of the images, the apparent bubble size does not change significantly due to competition between the radial expansion and the generation of additional magnetic fields. In the interaction region, the proton fluence structures are modified by the collision of the bubbles and the deformation of their magnetic field structures. The proton fluence in the interaction region is more complex than a superposition of proton deflection from either bubble, indicating that the path-integrated magnetic field structure is modified. The latter two images in both the symmetric and asymmetric configurations show that the proton pileup ring in the collision region is perturbed and flattened. This feature reflects the magnetic fields frozen into the plasma as it is being reshaped by the interaction with the opposing bubble. The asymmetric experiments, in particular, illustrate this deformation, and the stronger effect may be due to a more forceful collision.

The inference of proton-path-integrated magnetic field strength through the plasma from the beamlet deflection in a symmetric experiment is illustrated in Figure 4. Figure 4(a) shows the radiography images from which proton beamlet deflections (Figure 4(b)) and the path-integrated magnetic field strength (Figure 4(c)) are inferred. Though, as discussed above, the proton radiography images appear quite different on either side of the interaction region due to the geometry of the experiment, the magnitude and structure of proton beamlet deflection and, therefore, the magnitude and structure of the path-integrated magnetic field strength are approximately equal. In the interaction region of these parallel magnetic fields, no annihilation of magnetic flux is inferred, and a slightly increase in path-integrated magnetic field strength may occur, due to flux compression.

Maps of path-integrated magnetic field strength inferred from proton deflection are shown in Figure 5, directly illustrating the evolution and collision of magnetic field structures. The magnetic field structures are nearly identical on both sides in the symmetric experiments, as expected for identically-driven plasma bubbles. The maps show that path-integrated field strength and total magnetic flux increase throughout the 1-ns laser pulse as magnetic fields are continuously generated. The outer extent of the field structures expands radially at ~500 μm/ns. The field map is cut off at the top bubble as those proton beamlets are deflected entirely out of the field of view. A nearly azimuthally-symmetric profile of path-integrated magnetic field strength is observed at the plasma bubble perimeters, as has been observed in previous experiments.[11,16,20]

The interaction region of the plasma bubbles shows a slight enhancement of the path-integrated magnetic field strength, due to a weak pileup of magnetic flux. Lineouts of

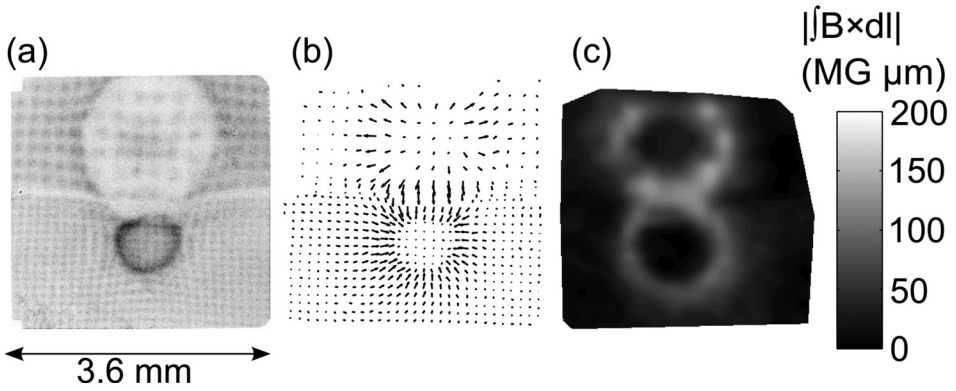

FIG. 4. (a) 15-MeV-proton radiography image, (b) beamlet deflection map, and (c) contour plot of the local magnitude of the path-integrated magnetic field strength inferred from beamlet deflections, for interacting symmetric plasma bubbles with parallel magnetic fields at $t_{int} = 0.4$ ns. These experiments show evidence of a slight enhancement of the path-integrated magnetic field strength in the collision region, possibly due to flux pileup.

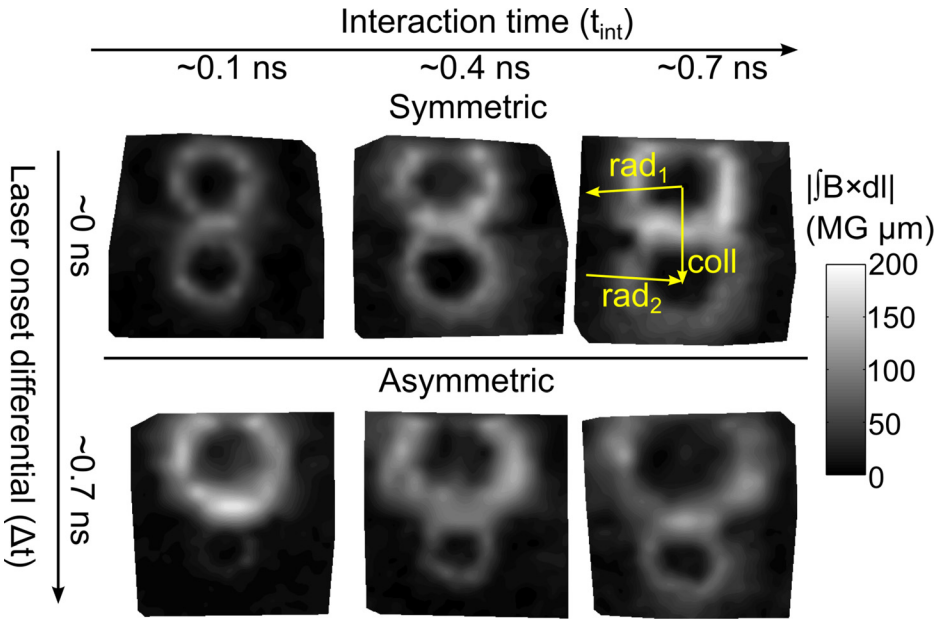

FIG. 5. Magnitude of path-integrated magnetic field strength inferred from 15-MeV-proton images at different times relative to the onset of the two interaction beams in parallel magnetic field experiments. As in Figure 3, the horizontal axis represents how long the two plasmas have been interacting for both symmetric ($\Delta t = 0$) and asymmetric ($\Delta t = 0.7$ ns) experiments. Lineouts are taken through the collision region ("*coll*") and radially around each individual bubble ("rad_1" and "rad_2") at 1.3 ns, as discussed in Figure 6.

path-integrated magnetic field strength (Figure 6) show that $|\int \mathbf{B} \times \mathbf{dl}|$ is enhanced and slightly narrower in the collision region of the plasma bubbles, in comparison to a mere superposition of radial profiles of $|\int \mathbf{B} \times \mathbf{dl}|$ from each bubble. This result indicates that a slight compression of magnetic flux is occurring, though the total magnetic flux ($\Phi = \int |\int \mathbf{B} \times \mathbf{dl}| dz$, where dz is the differential length along the lineout direction, perpendicular to the magnetic fields) is roughly conserved. As an example, in the symmetric experiments at $t_{int} = 0.4$ ns, the perimeter magnetic flux (as if integrated over rad_1 and rad_2) was $\Phi_{per.} = 87 \pm 11$ MG μm mm, while the flux in the interaction region (as if integrated over *coll*) was $\Phi_{int.} = 74 \pm 15$ MG μm mm. To within measurement uncertainty (including the random variation in $|\int \mathbf{B} \times \mathbf{dl}|$ around the perimeter of each plasma bubble), the net magnetic flux annihilated is consistent with zero. This result confirms that for the interaction of parallel magnetic fields, at a shear angle of ~0, magnetic reconnection does not occur and the magnetic flux is simply advected and compressed.

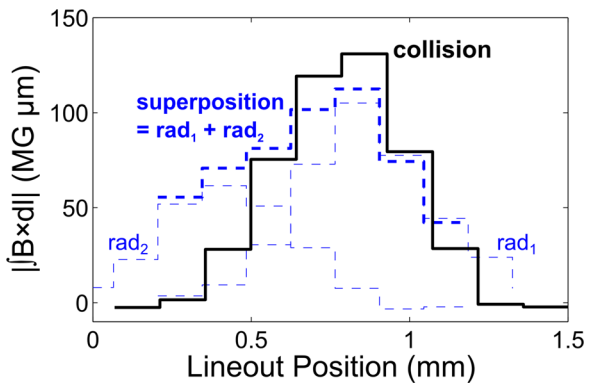

FIG. 6. Lineouts of path-integrated magnetic field strength ($|\int \mathbf{B} \times \mathbf{dl}|$) through the collision region and radially through each individual bubble, as indicated in Figure 3(b). The path-integrated magnetic field strength in the interaction region (thick solid line) is slightly greater and more sharply peaked than a simple superposition of radial profiles from individual profiles (thick dashed line), indicating that a collision of magnetic field structures has occurred.

IV. DISCUSSION

The plasma conditions at the interaction region illustrate that the plasma is in a regime where the magnetic fields are energetically subdominant and therefore are simply advected with the strong plasma flows and are susceptible to flux pileup. The perimeter of the plasma bubbles at the initial collision point in symmetric experiments is characterized by an electron density of $n_{e0} \sim 7 \times 10^{19}\,\mathrm{cm}^{-3}$ and an electron

temperature of $T_{e0} \sim 0.65\,\text{keV}$,[21] with a magnetic field strength of ~0.5 MG. Accounting for quasi-neutrality implies an average ion density (for a CH plasma with average ion charge $Z = 3.5$ and average ion mass $A = 6.5$) of $n_{i0} \sim 2 \times 10^{19}\,\text{cm}^{-3}$. As a result, the ratio of thermal pressure to magnetic pressure is $\beta \sim 8$. Additionally, the radial expansion velocity $V_r \sim 500\,\mu\text{m/ns}$ implies a ratio of ram pressure $(\frac{1}{2}\rho V_r^2)$ to magnetic pressure of $\beta_{ram} \sim 22$, so the magnetic field does not significantly perturb the dynamics and can be advected and compressed with the plasma fluid flow. As a consequence of this condition, equivalent to the flow velocity being much faster than the Alfvén speed based on these nominal conditions ($V_{A0} \sim 100\,\mu\text{m/ns}$), it is said that the interaction of magnetic fields is strongly driven. A typical magnetic Reynolds number is $Rm \sim 2000$, signifying that advection dominates diffusive processes, with the magnetic fields largely frozen into the plasma flow. These experimental conditions are in a regime of β, β_{ram}, and Rm comparable to strongly-driven laser-plasma magnetic reconnection experiments and, therefore, relevant to strongly-driven magnetic field interactions at the magnetopause.

In the related experiments driving the annihilation of anti-parallel magnetic fields, a factor of ~4 magnetic field amplification due to flux pileup has been predicted to account for the nominally super-Alfvénic rate of reconnection.[11] It is likely that in comparison to those experiments, the collision produced in these parallel magnetic fields experiments is somewhat weaker and at a more glancing incidence as the interaction point is farther from the laser focal spot and, consequently, farther from the generation of the bubble expansion and drive mechanism. The deformation of magnetic field structures is likely less forceful in this configuration than with two bubbles generated on the same side of a foil.

PIC simulations using the PSC code[11,12,22] were used to illustrate the expected magnitude of flux pileup in a 2D view of this collision of parallel magnetic fields. These PIC simulations, which model a 2D slice in the plane of the magnetic fields (parallel to the foil surfaces), were initiated based on hydrodynamic properties obtained from azimuthally symmetric 2D radiation-hydrodynamics simulations of a single laser-foil interaction. As was described in Ref. 11 for experiments using anti-parallel magnetic fields, in-plane profiles of density, temperature, and flow velocity were taken from 2D DRACO[23] simulations. Hydrodynamic quantities from DRACO simulations have been benchmarked against laser-foil experiments at a similar laser intensity ($\sim 10^{14}\,\text{W/cm}^2$).[24] Profiles of magnetic field strength were taken from 2D LASNEX[25] simulations. LASNEX-simulated path-integrated magnetic fields have been in good agreement with proton radiography measurements under similar conditions to the present experiments.[20] These profiles from an individual plasma bubble at the out-of-plane height where the two plasma bubbles collided were recorded at a time shortly before the collision and were used as initial conditions in the PIC simulations. The PIC simulations then modeled in 2D the interaction process of these colliding plasmas carrying annuli of parallel magnetic fields. The PIC simulations do not account for the continued laser drive or self-generation of magnetic fields and represent only a 2D slice through the 3D interaction geometry, but capture qualitatively the collision process and the resulting deformation of magnetic field structures.

The use of PIC, rather than hydrodynamic, modeling is especially important in the collision region, where the mean free path for ion-ion Coulomb collisions can become long compared to the size of the collision region. Based on plasma conditions described above, the mean free path for thermal ion-ion collisions within a single plasma bubble is ~800 μm, while the mean free path for ion-ion collisions between the colliding plasmas is of order ~50 cm, much longer than the ~mm scale of the collision region. In contrast, the length scales for collective plasma effects are shorter—the ion collisionless skin depth is ~40 μm, while the average ion gyroradius is ~25 μm. Therefore, it is expected that collisionless or collective effects are important, and these should be naturally accounted for in the PIC modeling.

Snapshots of the PIC-simulated magnetic field strength in the collision of parallel magnetic fields (Figure 7) illustrate the local amplification of magnetic field strength. The simulated magnetic field strength is enhanced in the collision region by a factor of ~3 as the ribbon of magnetic flux is squeezed by the opposing ram pressure between the two plasma bubbles. The total magnetic flux is conserved and the magnetic energy is enhanced. This result is qualitatively similar to the experimental results, where a modification and a slight enhancement of path-integrated magnetic field profiles occur, despite a conservation of total magnetic flux. However, the 2D simulations show a more substantial increase in the local magnetic field strength than is observed experimentally. This discrepancy is plausibly the consequence of 3D dynamics in the experiments, as plasma is allowed to flow in the out-of-plane direction perpendicular to the plane of the magnetic fields (i.e., perpendicular to the 2D plane of the simulations). In contrast, the simulations force a strong in-plane flux compression.

The lack of observed or simulated reconnection or annihilation of magnetic flux is expected, despite evidence of flux pileup. High-β plasmas, such as those produced in these experiments, are highly prohibitive of magnetic reconnection at small shear angles. It has been observed that reconnection is inhibited for sufficiently small magnetic shear angles or sufficiently high plasma β or $\Delta\beta$ across the current sheet, and the results of these experiments are consistent with observations and theory of magnetic field interactions at small shear angles, such as that occurs within the solar wind and at the magnetopause, where $\beta \sim 1$–5.[13] Importantly, the lack of magnetic flux annihilation demonstrates that these experiments constitute a

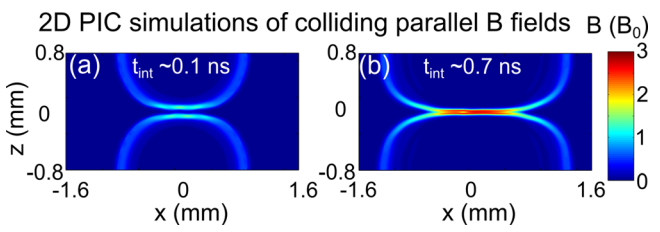

FIG. 7. Simulated magnetic fields in a 2D PIC simulation of colliding plasmas carrying parallel magnetic fields. These simulations show an amplification of the local magnetic field strength and a conservation of magnetic flux, in qualitative agreement with the data. However, the magnitude of pileup is stronger in the simulation.

test bed for studying flux pileup independent from (though relevant to) magnetic reconnection.

This innovative experimental design can be further optimized in order to generate plasma conditions and probe physics relevant to magnetic flux compression, and also to better understand strongly-driven magnetic reconnection experiments and similar astrophysical occurrences. In order to produce a more forceful collision and closely study flux pileup over a range of collision strengths, the relative position of the foils may be varied to generate different profiles of radial expansion velocity at the interaction plane. It is expected that by decreasing the spatial offset in the direction perpendicular to the two foils, such that the bubbles collide at a position closer to each foil surface where the radial flow velocity is greater, the interaction will be even more strongly driven, with a larger ratio of flow velocity to nominal Alfvén speed. In addition, increasing the lateral separation between the foils parallel to the foil surface will reduce the nominal density and nominal Alfvén speed at the collision point and allow for a test of the rate at which magnetic fields deform and pile up. Obtaining radiographs from the direction parallel to the foils will aid in discrimination of path integration effects and in determination of the 3D evolution of the plasma bubbles and their field structures.

V. CONCLUSIONS

In summary, proton radiography-inferred magnetic field data have been presented for the collision of parallel magnetic fields in laser-produced plasmas. These experiments demonstrate the deformation and possible pileup of magnetic field structures due to the hydrodynamic collision of parallel magnetic fields in a $\beta \sim 10$ plasma. The data show a slight compression of magnetic flux, but not as strongly as in 2D PIC simulations, as 3D dynamics of the plasma interaction may allow for a more glancing collision of magnetic fields. These experiments can be further optimized to study the amplification of magnetic fields as relevant to strongly-driven, flux-pileup-dominated magnetic reconnection in related laboratory experiments and in astrophysics.

ACKNOWLEDGMENTS

The authors thank the OMEGA operations and target fabrication crews for their assistance in carrying out these experiments and R. Frankel and E. Doeg for their help in processing of CR-39 data used in this work. This work was performed in partial fulfillment of the first author's PhD thesis and supported in part by U.S. DoE (Grant No. DE-NA0001857), LLE (No. 415935-G), NLUF (No. DE-NA0002035), and FSC (No. 5-24431).

[1]P. A. Sweet, in *Electromagnetic Phenomena in Cosmical Physics*, edited by B. Lehnert (Cambridge University Press, New York, 1958), p. 123.
[2]E. N. Parker, J. Geophys. Res. **62**, 509, doi:10.1029/JZ062i004p00509 (1957).
[3]J. Birn, J. F. Drake, M. A. Shay, B. N. Rogers, R. E. Denton, M. Hesse, M. Kuznetsova, Z. W. Ma, A. Bhattacharjee, A. Otto, and P. L. Pritchett, J. Geophys. Res.: Space Phys. **106**, 3715 (2001).
[4]T. Phan, L. Kistler, B. Klecker, G. Haerendel, G. Paschmann, B. Ö. Sonnerup, W. Baumjohann, M. Bavassano-Cattaneo, C. Carlson, A. DiLellis *et al.*, Nature **404**, 848 (2000).
[5]H. Ji, M. Yamada, S. Hsu, and R. Kulsrud, Phys. Rev. Lett. **80**, 3256 (1998).
[6]M. Yamada, R. Kulsrud, and H. Ji, Rev. Mod. Phys. **82**, 603 (2010).
[7]P. M. Nilson, L. Willingale, M. C. Kaluza, C. Kamperidis, S. Minardi, M. S. Wei, P. Fernandes, M. Notley, S. Bandyopadhyay, M. Sherlock, R. J. Kingham, M. Tatarakis, Z. Najmudin, W. Rozmus, R. G. Evans, M. G. Haines, A. E. Dangor, and K. Krushelnick, Phys. Rev. Lett. **97**, 255001 (2006).
[8]C. K. Li, F. H. Séguin, J. A. Frenje, J. R. Rygg, R. D. Petrasso, R. P. J. Town, O. L. Landen, J. P. Knauer, and V. A. Smalyuk, Phys. Rev. Lett. **99**, 055001 (2007).
[9]J. Zhong, Y. Li, X. Wang, J. Wang, Q. Dong, C. Xiao, S. Wang, X. Liu, L. An, F. Wang, J. Zhu, Y. Gu, X. He, G. Zhao, and J. Zhang, Nat. Phys. **6**, 984 (2010).
[10]Q.-L. Dong, S.-J. Wang, Q.-M. Lu, C. Huang, D.-W. Yuan, X. Liu, X.-X. Lin, Y.-T. Li, H.-G. Wei, J.-Y. Zhong, J.-R. Shi, S.-E. Jiang, Y.-K. Ding, B.-B. Jiang, K. Du, X.-T. He, M. Y. Yu, C. S. Liu, S. Wang, Y.-J. Tang, J.-Q. Zhu, G. Zhao, Z.-M. Sheng, and J. Zhang, Phys. Rev. Lett. **108**, 215001 (2012).
[11]M. Rosenberg, C. Li, W. Fox, I. Igumenshchev, F. Séguin, R. Town, J. Frenje, C. Stoeckl, V. Glebov, and R. Petrasso, Nat. Commun. **6**, 6190 (2015).
[12]W. Fox, A. Bhattacharjee, and K. Germaschewski, Phys. Rev. Lett. **106**, 215003 (2011).
[13]T. D. Phan, J. T. Gosling, G. Paschmann, C. Pasma, J. F. Drake, M. Oieroset, D. Larson, R. P. Lin, and M. S. Davis, Astrophys. J. Lett. **719**, L199 (2010).
[14]S. Chandrasekhar, *Hydrodynamic and Hydromagnetic Stability* (Clarendon Press, Oxford, England, 1961).
[15]T. R. Boehly, D. L. Brown, R. S. Craxton, R. L. Keck, J. P. Knauer, J. H. Kelly, T. J. Kessler, S. A. Kumpan, S. J. Loucks, S. A. Letzring, F. J. Marshall, R. L. McCrory, S. F. B. Morse, W. Seka, J. M. Soures, and C. P. Verdon, Opt. Commun. **133**, 495 (1997).
[16]R. D. Petrasso, C. K. Li, F. H. Seguin, J. R. Rygg, J. A. Frenje, R. Betti, J. P. Knauer, D. D. Meyerhofer, P. A. Amendt, D. H. Froula, O. L. Landen, P. K. Patel, J. S. Ross, and R. P. J. Town, Phys. Rev. Lett. **103**, 085001 (2009).
[17]C. K. Li, F. H. Séguin, J. A. Frenje, J. R. Rygg, R. D. Petrasso, R. P. J. Town, P. A. Amendt, S. P. Hatchett, O. L. Landen, A. J. Mackinnon, P. K. Patel, V. A. Smalyuk, J. P. Knauer, T. C. Sangster, and C. Stoeckl, Rev. Sci. Instrum. **77**, 10E725 (2006).
[18]M. J.-E. Manuel, A. B. Zylstra, H. G. Rinderknecht, D. T. Casey, M. J. Rosenberg, N. Sinenian, C. K. Li, J. A. Frenje, F. H. Séguin, and R. D. Petrasso, Rev. Sci. Instrum. **83**, 063506 (2012).
[19]J. A. Frenje, C. K. Li, F. H. Séguin, J. Deciantis, S. Kurebayashi, J. R. Rygg, R. D. Petrasso, J. Delettrez, V. Y. Glebov, C. Stoeckl, F. J. Marshall, D. D. Meyerhofer, T. C. Sangster, V. A. Smalyuk, and J. M. Soures, Phys. Plasmas **11**, 2798 (2004).
[20]C. K. Li, F. H. Séguin, J. A. Frenje, J. R. Rygg, R. D. Petrasso, R. P. J. Town, P. A. Amendt, S. P. Hatchett, O. L. Landen, A. J. Mackinnon, P. K. Patel, M. Tabak, J. P. Knauer, T. C. Sangster, and V. A. Smalyuk, Phys. Rev. Lett. **99**, 015001 (2007).
[21]M. J. Rosenberg, J. S. Ross, C. K. Li, R. P. J. Town, F. H. Séguin, J. A. Frenje, D. H. Froula, and R. D. Petrasso, Phys. Rev. E **86**, 056407 (2012).
[22]W. Fox, A. Bhattacharjee, and K. Germaschewski, Phys. Plasmas **19**, 056309 (2012).
[23]D. Keller, T. J. B. Collins, J. A. Delettrez, P. W. McKenty, P. B. Radha, B. Whitney, and G. A. Moses, Bull. Am. Phys. Soc. **44**, 37 (1999).
[24]S. X. Hu, V. A. Smalyuk, V. N. Goncharov, S. Skupsky, T. C. Sangster, D. D. Meyerhofer, and D. Shvarts, Phys. Rev. Lett. **101**, 055002 (2008).
[25]G. B. Zimmerman and W. L. Kreur, Comments Plasma Phys. Controlled Fusion **2**, 51 (1975).